

# Runout transition and clustering instability observed in binary-mixture avalanche deposits

**Roberto Bartali<sup>1</sup>, Gustavo M Rodríguez Liñán<sup>2</sup>, Luis Armando Torres-Cisneros<sup>3</sup>, Gabriel Pérez-Ángel<sup>3</sup> and Yuri Nahmad Molinari<sup>2</sup>**

<sup>1</sup> Facultad de Ciencias, Universidad Autónoma de San Luis Potosí, Salvador Nava 5, 78290, San Luis Potosí, Mexico.

<sup>2</sup> Instituto de Física, Universidad Autónoma de San Luis Potosí, Salvador Nava 5, 78290, San Luis Potosí, Mexico.

<sup>3</sup> Departamento de Física Aplicada CINVESTAV-IPN, Unidad Mérida, Apartado Postal 73 Cordemex 97310. Mérida, Mexico.

E-mail: rbartali@uaslp.mx robertobartalin@gmail.com

**Abstract.** Binary mixtures of dry grains avalanching down a slope are experimentally studied in order to determine the interaction among coarse and fine grains and their effect on the deposit morphology. The distance travelled by the massive front of the avalanche over the horizontal plane of deposition area is measured as a function of mass content of fine particles in the mixture, grain-size ratio, and flume tilt. A sudden transition of the runout is detected at a critical content of fine particles, with a dependence on the grain-size ratio and flume tilt. This transition is explained as two simultaneous avalanches in different flowing regimes (a viscous-like one and an inertial one) competing against each other and provoking a full segregation and a split-off of the deposit into two well-defined, separated deposits. The formation of the distal deposit, in turn, depends on a critical amount of coarse particles. This allows the condensation of the pure coarse deposit around a small, initial seed cluster, which grows rapidly by braking and capturing subsequent colliding coarse particles. For different grain-size ratios and keeping a constant total mass, the change in the amount of fines needed for the transition to occur is found to be always less than 7%. For avalanches with a total mass of 4 kg we find that, most of the time, the runout of a binary avalanche is larger than the runout of monodisperse avalanches of corresponding constituent particles, due to lubrication on the coarse-dominated side or to drag by inertial particles on the fine-dominated side.

*Keywords:* binary avalanches, granular flows, granular clustering, segregation process  
*Submitted to:* *J. Geophys. Eng.*

## 1. Introduction

Rock avalanches and geophysical granular flows have been broadly studied in order to understand the potential risks they represent and the modifications they make on the landscape. They mobilize millions of cubic meters of rocks, with sizes ranging from microns up to tens of meters, running at velocities that, in some cases, are faster than 100 km/h (Robinson *et al* 2015, Clavero *et al* 2002, Fauque and Strecker 1988, Siebert 1984, Ui 1983). Since their behaviour depends on a myriad of parameters, such as particle-size distribution, hardness, textural characteristics, friction and restitution coefficients, kind of triggering event, and the environment in which they develop, travel, and deposit, they are very complex phenomena, which are difficult to predict and/or to be modelled. Any interstitial fluid, like hot gas (such as in pyroclastic density currents) or water (like in mudflows and lahars), also plays a fundamental role in the flow behaviour, due to lubricating effects, which, in turn, increase the associated risk. For this reason, experiments with model particles and simple geometries are performed at laboratory scale in order to understand the main features of the avalanching process. In this simplifying spirit, monodisperse avalanches and the role that basal friction has on the runout have been systematically studied, *e.g.*, by Goujon *et al* (2003). They found a minimum basal friction, which depends on particle size, and developed a simple model to determine how the geometric parameters of the rough base modify the runout of the avalanche.

Several groups have studied the origin of the scaling laws that describe the length and height of the deposit as a function of the initial conditions (Pouliquen 1999, Andreotti *et al* 2002) and coefficients of restitution of materials (Campbell 2006). Other observations relate the distance travelled by avalanches with the topography of the terrain or with the presence of model forests at the slope change (Yang *et al* 2011). Several other mechanisms may affect the mobility of avalanches, for example, dynamic fluidization (Huerta *et al* 2005), fluid-pore-pressure increment, or ball-bearing effects induced by the presence of fine particles within large inter-particle voids (Pacheco-Vázquez and Ruiz-Suárez 2009, Hungr and Evans 2004). Several hypotheses regarding the mechanisms that lead to long runouts and the mobility of rock avalanches are summarized in Charrière *et al* (2015) and references therein. Increased mobility of avalanches containing large and fine grains is also observed in numerical simulations (Linares-Guerrero *et al* 2007). In summary, particle-particle and particle-base interactions have been the object of thorough research to shed some light on the problem of how the multiple factors of a real avalanche are related with the final developed deposit and its runout, height and length, in order to better predict the risks they could represent.

During their development, avalanches present an irregular flow characterized by an intermittent motion

(stick-slip) and formation of density waves. Van Gassen and Cruden (1990) developed a model in which they describe the increments in runout due to intermittent deposition of a dry granular flow. Later on, some stick-slip motion of the flow down a slope was reported by Bartali *et al* (2015). They developed a medium-size, densely instrumented experimental flume (Bartali *et al* 2012, Bartali *et al* 2015) and found evidence of this intermittent behaviour in polydisperse, dry granular flows and an increment of the affected area through the ejection of ballistic projectiles.

Stick-slip motion will very likely produce reminiscent features in the final deposit. Seeking for these reminiscences, Paguican (2014) performed analogous model experiments aimed to reproduce and understand the origin of hummock formation and the dynamics of spreading and aggregation. The intermittent motion causes concomitant faulting and sliding zones that will finally form the characteristic elevations and mounds scattered on top of the deposition area. In field observations, intriguing hummocks, constituted mainly by coarse grained rocks and situated beyond the avalanche front, have been described and interpreted by Clavero *et al* (2002).

On increasing complexity, mixtures of two particle sizes in different proportions have also been investigated. In those cases, ubiquitous segregation occurs in different forms: levees, vertical segregation by kinetic sieving, inertial dispersion of ballistics, etc. Several authors report a non-monotonic behaviour of the runout (mobility) of avalanching masses as a function of fine-particle content (Phillips 2006, Yang 2015, Moro 2010, Goujon *et al* 2007). Likewise, Kokelaar *et al* (2014) used rough, irregularly shaped materials mixed with smooth, rounded grains in order to describe how both materials interact with each other and with the base while they flow down the slope. They observed a levee formation that guides the avalanche by channelling or confining the flow of fine grains by the so-called “outline effect”. Similarly, Kokelaar *et al* (2014) observe the growth of the runout up to a maximum occurring at a critical proportion of fine particles.

In summary, a critical fine-particle content is responsible for the maximum mobility of the avalanche by lubricating interactions among large particles and between large particles and the base, and it has been well established for binary avalanches. All these reported data suggest that the runout is a continuous function of the fine content. However, in this work we report that each size component has its own very well differentiated runout. During the flow, the avalanche spreads out and segregates by size, continuously changing the effective composition of the mixture in different locations. The avalanching mass is thus a non-homogeneous mixture of two dynamically changing species along the channel until it completely stops. The different runouts of each species would lead, in the case of a complete separation during the flow, to a two-folded runout value or a discontinuous transition of the runout as a func-

tion of fine-particle content, never observed or reported before.

The main objective of this work is to systematically address the runout value in binary avalanches with enough contrast in grain-size species, finely exploring the behaviour of the avalanche runout around the critical value where the runout reaches its maximum, modifying the fine-particle content in steps as small as 2.0%. Changes in runout account for a different rheological behaviour and could help in developing risk-management strategies and in providing a more accurate interpretation of past geological flows from their deposits. The purpose of our experiments is to understand the interactions between dry, irregular, natural particles running down a flume. Particle-particle interactions (collisions and friction) may be changing dynamically, so the microscopic (grain-level) behaviour, must influence the macroscopic (flow-level) behaviour and, hence, the velocity of the flow and its energy dissipation per unit time. The final runout and the morphology of the deposit must be a direct consequence of the interactions of all the grains.

## 2. Experimental setup

We built a laboratory medium-scale (2.5-m long, 15-cm wide), variable-tilt ( $0^\circ$  to  $45^\circ$ ) flume (figure 1a), followed by a 1.8-m-long and 1.2-m-wide, horizontal deposition area. Both the flume and the deposition area were built using 15-mm thick, smooth, medium-density fibreboard (MDF) sheets. The flume base was covered by a hard, smooth Formica sheet in order to reduce the basal friction, while the deposition area was covered with a vinyl paint to obtain some roughness. The walls in both sections consisted of a 15-cm-height, 6-mm-thick, transparent, tempered glass. An open-frame, metallic structure ( $50\text{ cm} \times 50\text{ cm} \times 2.5\text{ m}$ ) was employed to hold the flume at the desired tilt. A manual gate was placed 2 m up-stream (from the break in slope) in order to accumulate the granular material and start the avalanche with zero velocity. This gate was connected to a micro-switch that allowed the automatic trigger of a high-resolution ( $2208 \times 1244\text{ px}$ ), high-frame-rate (120 fps) video camera (Sony HDR-HR150).

We also painted a square grid, 5 cm in side, over the base of the deposition area to allow a better scaling and measurements of the runout and the morphology of the avalanche deposit. For all the experiments, we used irregular, rough, natural particles collected in the same area to ensure uniformity of density ( $2.6\text{ g/cm}^3$ ), morphology, and textural features (figure 1b). This material (andesite clasts from a deposit of a block and ash flow at Nevado de Toluca volcano in Mexico) was carefully sieved in order to obtain grain-sizes classes, based on the Wentworth (1922) scale, from  $-4\text{ phi}$  (16 mm) to  $4\text{ phi}$  (0.0625 mm) mean grain diameter. We also sieved the granular material to obtain intermediate grain-size classes:  $-1.5\text{ phi}$  (3 mm),

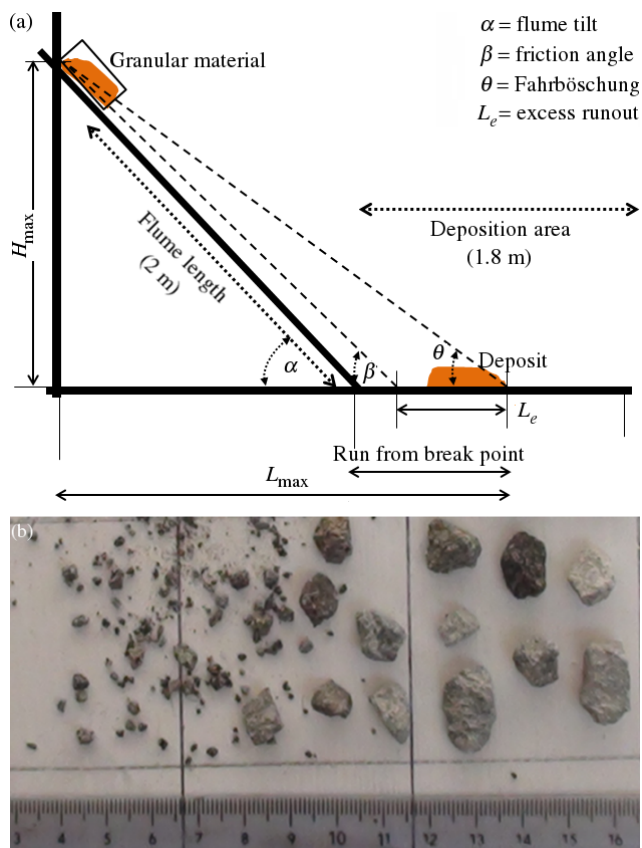


**Figure 1.** (a) Schematic diagram of the experimental flume. The parameter definitions are given in the text when used. The flume tilt,  $\alpha$ , can be set from  $0^\circ$  to  $45^\circ$ . (b) Example of the irregular volcanic particles used to perform the experiments.

$-0.5\text{ phi}$  (1.5 mm) and  $1.5\text{ phi}$  (0.375 mm). The total mass obtained for each granular class was 4 kg. We used standard sieves, so a monodisperse set of grains means that it contains all the grains that pass through the mesh. In order to ensure a better grain-size selection, the loads of grains were sieved twice.

## 3. Method

Different granulometric classes were characterized by determining their repose angle and static friction coefficients. For doing so, collapsing-granular-column experiments and tilted table tests were performed ten times for each particle size. For repose angle determination, an 8-cm-radius tube was filled with 469 g of granular material, and the tube was slowly and vertically removed in such a way that the granular column collapses into a conical mound. The true shape of the mound is shown in figure 2, where three different angles are defined. The repose angle is represented by  $\sigma$ , whereas  $\beta$  and  $\varepsilon$  represent respectively the smooth slope of the material that collapses after the pile formation and the full-pile angle related to  $\sigma$  and  $\beta$ . Static friction coefficients were determined by gluing a layer of granular material on

the base of a wood slab, which was weighted and checked for the critical angle at which it starts sliding down over a smooth metallic plate.

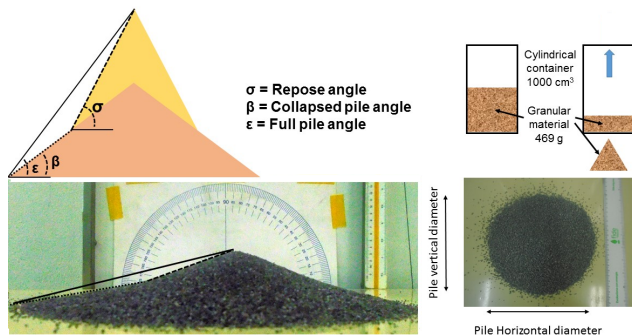


**Figure 2.** Experimental setup and definition of the angles measured after the formation of the pile.

Static-friction angles and repose angles are plotted in figure 3 as a function of the granulometric class, phi, showing an increasing trend as the particle size diminishes.

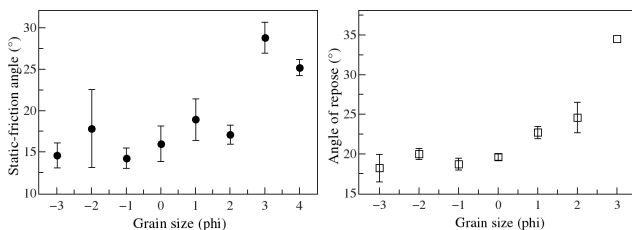


**Figure 3.** (a) Static-friction angle in tilted-table experiments as a function of the granulometric class phi. (b) Repose angle as a function of the granulometric class.

We performed experiments aimed to understand the behaviour of dry avalanches containing only particles of two different sizes mixed together. We combined different grain classes maintaining the total mass of the granular material constant (4 kg) and then changing the relative proportion of each class. The first run was always performed with the coarsest grained sample, while the second was the finest grained one, both cases having 4 kg of particles, as stated before. This methodology rules out the possibility of contamination with fine particles of larger grains masses. Before each experiment, we slowly poured all the grains (previously sieved) in a bucket, slowly turning with a ladle, trying to get the best mixture. We performed experiments with the flume tilted at 32° and at 37°, maintaining, in all cases, the deposition area horizontally. The set of experiments is summarized in table 1.

The video camera was placed in front of the flume and perpendicular to the deposition area, in order to have almost all the flume and part of the deposition area in the field of view. The camera was triggered automatically by a micro-switch connected to the gate, which was used to

**Table 1.** Set of the different experiments performed.

| Flume tilt (degrees) | Coarse grains phi (mm) | Fine grains phi (mm) |
|----------------------|------------------------|----------------------|
| 32                   | -3 (8)                 | 2 (0.25)             |
| 32                   | -2 (4)                 | 2 (0.25)             |
| 32                   | -1 (2)                 | 2 (0.25)             |
| 37                   | -3 (8)                 | 1.5 (0.375)          |
| 37                   | -1.5 (3)               | 1.5 (0.375)          |

start the avalanche. Several markers on the flume and on its walls and the grid painted on the deposition surface helped to measure the velocity and the horizontal displacement of the granular flow body and that of scattered high-velocity-ejected particles. After each experiment, we sieved the granular material, weighted the amount to be used in the next run, and mixed all the grains again. In order to ensure that the experimental conditions were almost the same for all the experiments, we carefully cleaned the flume and the deposition area, because fine and very fine grains, in small quantities, increase the mobility of the avalanche, as we will show in the next section. The flume was cleaned each time, first with a brush and, if very small particles were found on the base or walls, with a wet cloth or running water. If this was the case, the flume was dried with a hairdryer. The granular material used in each experiment was always from the same initial set of 4 kg, in order to maintain the same textural and morphological characteristics.

All the materials selected for the flume (Formica and tempered glass) and the deposition area are almost static-free. We performed several tests in order to find out which grain size was the most affected by electrostatic attraction, sprinkling the flume at several tilt angles. It turned out that only 62- $\mu\text{m}$  (4 phi) and finer particles were significantly adhered to the base and the walls of the flume; consequently, we chose to not perform experiments with those grain sizes.

#### 4. Results and discussion

In the following sections, we will discuss the results of the experiments and compare them in order to show that they are consistent. We will show that segregation of particles depends on particle size and content ratio. Finally, we propose that granular clustering is the origin of the deposit morphologies observed experimentally. We also propose that granular clustering can be an alternative or an associated process involved in the hummock-formation mechanism for which there are several explanations in the literature (Peguican *et al* 2014, McColl and Davie 2011, Clavero *et al* 2002, Glicken 1996, Siebert 1984, Ui 1983).

#### 4.1. General description of the deposit

In figure 4a, a typical deposit of a binary avalanche is shown. In this case, the coarsest particles measure 8 mm (55% by mass), while fine grains are 0.375 mm (45% by mass). Clearly, the deposit is segregated, presenting a region of only fine particles (pink), a region with a mixture of coarse and fine particles (the finest at the bottom and the coarsest on top) and a region in which just coarse particles are deposited (dark gray). In some cases, a gap opens up between the mixed and the coarse-particle regions. If the mobility of the avalanche is not large enough to overpass the break in slope and to deposit on the horizontal deposition area, the fine-particle deposit and part of the mixed-particle deposit remain on the flume, as can be seen in figure 4b. In this deposit, the largest particles have a mean diameter of 4 mm (62.5% by mass), and the finest ones measure 0.25 mm (37.5% by mass).

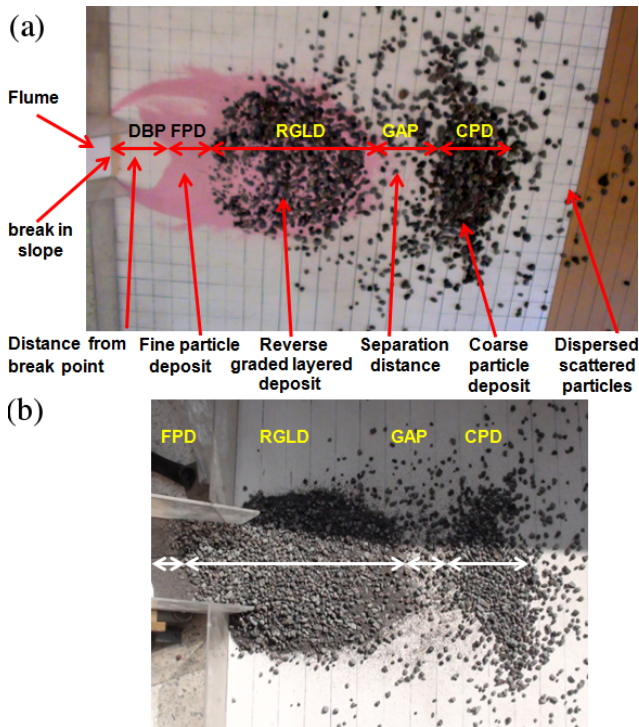


**Figure 4.** (a) Example of a binary avalanche deposit consisting of 2.2 kg of 8-mm (black) particles mixed with 1.8 kg of 0.375-mm (pink) particles. The flume tilt was set to 37°. (b) Example of a binary avalanche deposit consisting of 2.5 kg of 4-mm (large, gray) particles mixed with 1.5 kg of 0.25-mm (small, gray) particles. The flume tilt was set to 32°. There are clearly three different deposits, due to the segregation processes occurring during the avalanche, the collision against the break in slope, and the travel of particles on the horizontal deposition area.

The characteristic lengths of the different parts of the deposit (see figure 4) are defined as the “distance from break point” (DBP), which is measured from the break point to the tail of the fine-particle deposit. The fine-particle deposit length (FPD) refers to the distance from DBP to the point in which a mixture of particles can be

seen. At this point starts the mixed deposit, which actually consists of two perfectly reverse-graded layers (RGLD), and its length is measured to the point in which particles are no longer in mutual contact. Between the mixed-particle deposit and the coarse-particle deposit (CPD) there are scattered particles forming a gap (GAP), consisting of a low-density cloud of coarse particles. This low-density cloud of scattered particles ends where the density of particles suddenly increases, forming a cluster of coarse-particle deposit (CPD). Outside this last region, particles are scattered and form a large V-shaped cloud. The distance from the break in slope to the tip of the coarse-particle deposit will be called hereafter “run from the break point” (RBP). All these lengths are measured on the horizontal deposition area along the symmetry axis of the flow and will be very important at describing the complex phenomenology of the granular, binary-mixture avalanches.

#### 4.2. Detailed deposition sequence

In figure 5, a sequence of pictures of the final deposits for ten different fine contents is shown. The avalanche contained a mixture of 8-mm particles (large, black) and 0.375-mm fine particles (pink). These experiments were performed with a flume tilt of 37°. The fifth pictured deposit, corresponding to 55% of large particles and 45% of fine clasts, is the one shown previously in figure 4a.

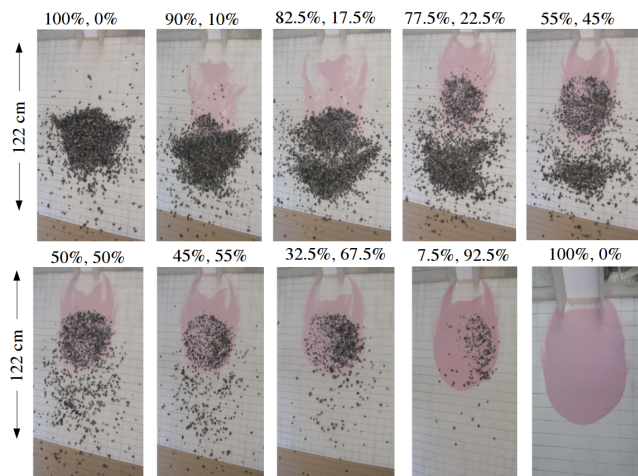


**Figure 5.** Sequence of deposits created by the binary avalanche, containing 8-mm (gray) and 0.375-mm (pink) particles. Fine-particle content in the mixture increases from left to right. A dramatic change in the deposit morphology is clear when the fine-particle content increases from 45% to 50%. The deposit suddenly retreats. The grid on the horizontal deposition area is 5 cm × 5 cm.

It is interesting to observe that, when the mixture contains 55% of large particles and 45% of fine particles (see the fifth and sixth pictures in figure 5), the deposit shows a bi-modal structure; in some cases, there is a large cluster of coarse particles at the distal part of the deposit and, in other cases, a very small one. This double behaviour

can be obtained by changing the content of fines by a factor of 3% or less.

The sequence of deposits shown in figure 6 was produced by an avalanche of 4-mm particles (dark gray) mixed with 0.25-mm ones (light gray). The content of fine particles in figure 5 and figure 6 increases from left to right, growing from 0% to 100% by mass. The sudden change in the deposit morphology and, hence, the retreat of the runout, is obtained when the fine-particle content in the mixture changes from 43.75% to 50%, when the large cluster at the distal part of the deposit suddenly retreats (see the fifth and sixth pictures in figure 6).

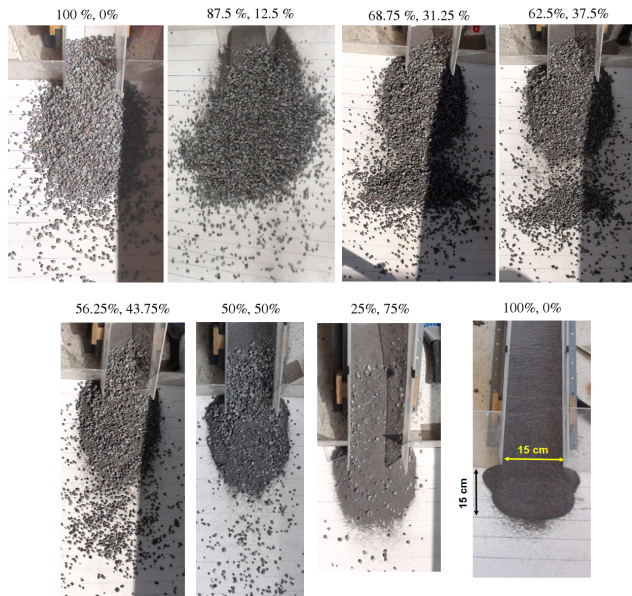


**Figure 6.** Sequence of deposits created by the binary avalanche containing 4-mm (large, gray) and 0.25-mm (small, gray) particles. The fine-particle content in the mixture increases from left to right. A dramatic change in the deposit morphology is clear when the fine-particle content is increased from 43.75% to 50%. The deposit suddenly retreats. The grid on the horizontal deposition area is 5 cm  $\times$  5 cm.

From the analysis of figures 5 and 6 and all the experiments listed in table 1, we get the different plots shown in figure 7, in which the run from break point (RBP) is depicted as a function of fine-particle content. It can be seen that, for a null fine content, the coarse particles form a single, large cluster surrounded by scattered particles towards the front. When a few percent of fines are added to the mixture, the deposit separates into three clearly defined zones: an only-fine-particle deposit, a mixed deposit and an only-coarse-particle deposit. It is worth to note that the mixed deposit always consists of two reverse-graded layers, where fine grains are at the bottom and coarse particles are on top of them.

An increment in the run from break point (RBP) is observed, and its value depends on the grain-size ratio and the flume tilt. This trend continues until the RBP reaches an almost constant value. As more fine particles are added to

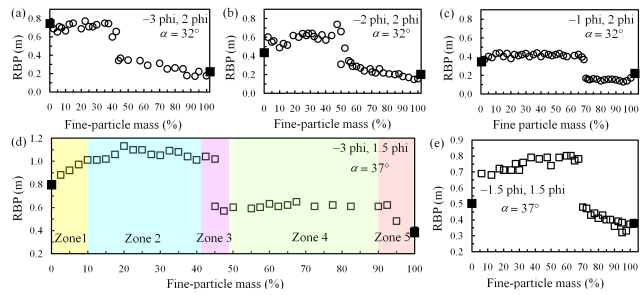


**Figure 7.** Total distance travelled by the avalanche on the horizontal deposition area—“run from break point” (RBP)—plotted as a function of the fine-grain content (%). Three results—(a), (b), and (c)—with the flume tilted 32° and two other—(d) and (e)—for the flume tilted 37° are shown. In all cases, a sudden change in the RBP length is observed. The amount of fines needed to produce this transition depends on the grain-size ratio in the granular flow mixture. Five different zones can be recognized in all plots. For clarity, they are highlighted in plot D: Zone 1, RBP increment; Zone 2, RBP almost constant; Zone 3, RBP transition; Zone 4: RBP almost constant; Zone 5, RBP decrement or almost constant. The black filled square (on each plot) is the run from break point of the large-particle monodisperse avalanche (left side) and that of the small particles (on the right side).

the mixture, the pure-fine deposit is more clearly defined and the coarse-particle deposit separates from the mixed deposit, leaving a gap full of scattered particles in between. Further addition of fine particles induces the dilution of the distal, large cluster containing only coarse particles into one or more small clouds of particles (small clusters).

A small (around 5–7%) increment in the fine-particle content in the mixture produces a sudden reduction in the RBP, and both the gap and the clusters of coarse particles disappear. If the fine-particle fraction is still increased, the few coarse particles in the flow are not able to overcome the fine deposit, thus getting stuck over what would be, otherwise, the fine deposit, forming a mixed deposit. However, some coarse particles abandon this last deposit to conform the scattered cloud of particles far from the massive deposit. The trend observed in the three cases for which the flume was tilted 32° is similar to that when the flume tilt was set to 37°. For this reason, we decided to show only one result for each flume tilt and discuss them in general terms.

It should be pointed out that avalanches constituted only of fine particles are deposited mainly on the slope, while those constituted of coarse particles are deposited on the horizontal deposition area, consistently with the viscous-like and inertial regimes described above. In fact, the abrupt change in slope could induce the development of sudden internal passive pressures, due to air compression during the deposition process.

It is clear that a small percentage of fine particles increases the runout and, hence, the horizontal travel (RBP) of the avalanche before it settles down and deposits. We attribute this behaviour to lubrication produced by fine particles among large particles and between the avalanche

body and the flume surface. On the other hand, a large amount of fine particles acts as a “sand-trap” for coarse ones. Regardless of the grain size, they always get stuck inside the massive avalanche and the deposit of fine particles. A large particle colliding against thousands of smaller particles loses suddenly almost all its kinetic energy. As the radii fraction tends to unity, the contrast in the flow regimes is reduced, the separation of the deposits become more difficult, and the whole behaviour will be the one of a monodisperse avalanche.

We should highlight that we have selected mixtures with coarse particles larger than 1 mm and fine particles with less than 1 mm, mean diameter. This is because the behaviour of monodisperse avalanches containing particles larger than 1 mm is very different to that corresponding to granular flows containing particles smaller than this size. We have experimentally determined (see figure 8) that the coarse-grained ( $> 1$  mm), monodisperse-avalanche travels in an inertial-like regime, and its RBP (and the corresponding runout) grows proportionally to grain size, showing an increment five times larger, or more, for a 16-fold increment in particle diameter.

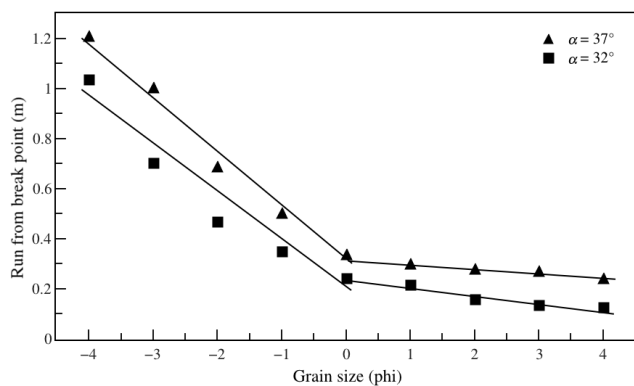


**Figure 8.** Run from break point (RBP) plotted as a function of grain size for monodisperse avalanches. Each point is the mean value after running five experiments. The mass of grains in each avalanche is 4 kg. A kink can be seen in both trends at a grain size of 1 mm. The RBP for particles larger than 1 mm increases proportionally to grain size, while for particles smaller than 1 mm it remains almost constant. This plot shows a dramatic change in the behaviour of the avalanche from an inertial regime (particles larger than 1 mm) to a viscous-like regime (particles smaller than 1 mm), as discussed in text.

For particles larger than 1 mm, the kinetic energy acquired at the expense of the potential-energy loss is higher than the energy lost by friction and collisions. On the other hand, monodisperse avalanches containing grains smaller than 1 mm behave similar to a viscous-like flow, maintaining a much slower increase (they shows a less-than-twofold increment for a 16-fold increment in particle diameter) in the runout and RBP values, regardless of the grain size. In this case, the energy lost by dissipative processes (friction and collisions) is higher than the kinetic-energy increment due to their movement down-slope. This

is because, as grain size is reduced for the same mass, the number of particles increases as the cube of their radius, so the number of mutual collisions and contacts between particles also increases at the same proportion.

We have further tested the previous hypothesis by performing 2D molecular-dynamic simulations of dimers, consisting of overlapped discs, and accounting for the instantaneous dissipated power as shown in figure 9 (simulation details will be published elsewhere). In this figure, the total, instantaneous dissipated power is plotted as a function of time for different number of particles,  $N$ , maintaining the total mass constant. Time axis spans from the triggering of the avalanche to the moment at which the avalanche front reaches the deposition zone. As it can be seen, the dissipated power is always larger for smaller grain sizes, in agreement with the aforementioned hypothesis. Having a larger number of particles implies more collisional events and, hence, more power dissipated by finer grains. This is consistent with the experimental results shown in figure 8, in which runout decreases monotonically with decreasing grain size.

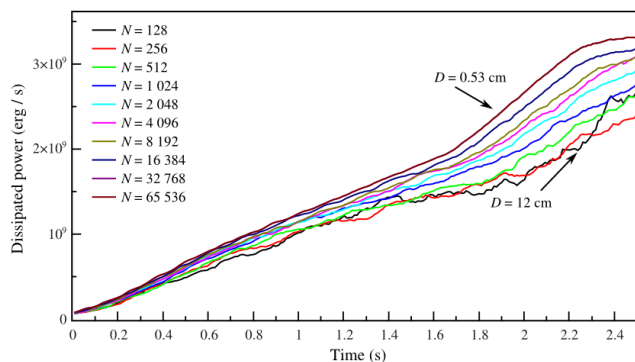


**Figure 9.** Instantaneous dissipated power of the whole simulational 2D avalanche of dimers as a function of time for different number of dimers, keeping the total avalanching mass constant.

In figure 3, the repose angle as a function of grain size—a static measure—shows consistency with the dynamic response shown by RBP in the sense that friction is more important for small grains than it is for large ones. However, the dynamic response measured trough RBP involves the acceleration stage, as well as the deceleration produced at the break in slope, which is a much more complex phenomenon.

#### 4.3. Comparison of experimental results

In this section we show the results obtained after running the avalanches with a change of the fine-particle content of 2.5% in each step (in almost all cases). This finely tuned exploration of the run from the break point as a function of the fraction of fine particles in the mixture was made because a sudden transition was detected during the experiments. As can be seen in figures 5, 6, and 7, as the

proportion of fine grains increases from zero to one, several behaviours can be noted. In all plots in figure 7, the run from the break point (RBP) of mixed avalanches is plotted. Five different regions can be observed in all plots depicted in figure 7 but, for clarity, we have highlighted them only in figure 7d. In some cases, differences among regions are too subtle to be discerned. However, the main transition reported in this paper is always present and is notoriously sharp.

First, at very small fine percentages, around 5–15%, after the first coarse-grained, monodisperse-avalanche RBP value (the first black square), a growing tendency of the RBP as a function of fine-particle content is recorded (depicted as zone 1), followed by a much slower growth rate (zone 2), until a sudden step-function-like fall of the RBP occurs (zone 3). After this sudden transition, a slow decreasing of the RBP follows (zone 4) and, finally, for all cases, except the one shown in figure 7d. This tendency continues until the value of the RBP of the fine-grained, monodisperse avalanche is reached, which is always less than or very similar to the last RBP of a mixture. This tendency of the RBP occurs when the proportion of fine particles is larger than 90% by mass (zone 5). The observed transition in zone 3 produces larger changes in the RBP for larger particle-size ratios and occurs at smaller fine-particle contents for larger size ratios, as it can be seen in table 2. The fourth column in table 2 shows that the critical content of fine grains shifts inversely with the grain-size ratio for a constant flume tilt. It is worth to note that the transition width is, in all cases, close to a 7%, or less. This variation in fine-particle content of the mixture was observed for experiments performed at all flume tilts.

The separation between mixed- and coarse-grain deposits increases linearly with the fine-particle content until it falls abruptly again to zero (the two deposits can no longer be distinguished). The run from the break point is increased due to the separation of the avalanche into two fronts: an inertial one (coarse) and a more viscous-like one (mixed). The sudden transition occurs at the point in which the content of fine particles is so large (there is a small number of coarse particles) that coarse particles get trapped between the fine ones, and the few ones that can overcome the fine-particle deposit cannot form a well-defined deposit. The beginning or the end of a deposit is always measured from the point in which the density of scattered particles grows, forming large ( $> 1/3$  of the flume width) clusters, allowing the stability of superimposed particles in two or more layers. The way in which the tip and tail of the deposits are defined is critical to understand the discontinuous character of the observed transition.

The addition of few coarse grains to a mixture composed mostly of fine particles only traps these coarse grains within the massive fine-particle deposit. The avalanche behaviour is now dominated by the viscous-like nature of the flow of fine particles. Further addition of

coarse particles provokes that some of these much more inertial grains can overcome the deposit of fine and mixed particles, which can be found randomly scattered beyond the main deposit, forming a disperse cloud. As this process of increasing the coarse fraction is continued, more and more particles are added to the coarse-particle cloud, until they start clustering together by inelastic interactions.

The density of the scattered cloud of coarse particles increases until a critical density is reached and large clusters form. The first cluster stops the particles coming from the avalanche and the just-formed coarse deposit can grow as more coarse particles are added to the mixture. This is an inertial deposit, and the subsequent behaviour of the run from the break point will be dominated by inertial particles. In this way, one may say that the discontinuous transition of the RBP at a critical content of fine grain is actually the separation of the deposit into two main deposits: the one of mixed particles and the cluster of scattered, coarse particles that condense to form the coarse-grain deposit at the very front. Before the onset of clustering there is not a well-defined coarse deposit, and just a diffuse cloud of randomly distributed, coarse particles can be identified. Thus, the massive front of the deposited material is composed of coarse particles trapped by the fine-grain deposit.

At this point, let us mention, for the sake of clarity, a few words on clustering and inelastic-collision-driven transitions in granular matter. “Inelastic collapse” (Goldhirsh and Zanetti, 1993) is a phenomenon in which simulations of granular gases cooling down by inelastic collisions seems to stop. The apparent stall of the simulation occurs because when two particles approach, sandwiching a third particle, they cause this third particle to perform a diverging number of collisions per unit time. The collision routine is thus invoked a diverging number of times but the relative positions of the particles involved in the formation of this cluster evolve very slowly as if the simulation were halted. On the other hand, “granular clustering”, closely related to inelastic collapse, is the phenomenon in which the restitution coefficient depends on the relative collision velocity (as in the case of real grains) and has been reported in quasi-two-dimensional granular gases as responsible for segregation in compartmentalized granular gases (Olafsen and Urbach 1998, Sapozhnikov *et al* 2003, Bordallo-Favela *et al* 2009, Perera-Burgos *et al* 2010, Mikkelsen *et al* 2002, Mikkelsen *et al* 2005). In the clustering instability, the power dissipated in the collisions grows as the inter-particle separation decreases, because the number of collisions diverges when they come closer. In this sense, as more particles cluster together, it is easier for them to trap particles from the cloud within the cluster. Thus, clustering is a self-enhanced process.

The formation of two different deposits separated by a gap, shown in figures 5 and 6, could be explained as a consequence of a clustering process. This process produces the second well-defined deposit transversal to

**Table 2.** Run from break-point transition for all experiments.

| Flume tilt (degrees) | Transition particle diameter (ratio) | $\Delta$ RBP (m) | Mean fine mass transition content (%) | Fine content transition width (%) |
|----------------------|--------------------------------------|------------------|---------------------------------------|-----------------------------------|
| 32                   | 32                                   | 0.41             | 43                                    | 7                                 |
| 32                   | 16                                   | 0.43             | 48                                    | 7                                 |
| 32                   | 8                                    | 0.25             | 68                                    | 5                                 |
| 37                   | 21.3                                 | 0.42             | 45                                    | 3                                 |
| 37                   | 8                                    | 0.31             | 68                                    | 7                                 |

the flow direction of the avalanche, due to the fact that local stresses are of compressive nature. In other words, no extensional stresses are possible due to discontinuous granular interactions among grains in this horizontal deposition area. This clustering-driven formation of a separated deposit and small, dispersed clusters, in our lab-scale experiments, recalls the hummocks observed in natural rock avalanches.

It should be remarked that avalanche-runout increments due to fine particles have been reported previously (Kokelaar *et al* 2014, Goujon *et al* 2007, Phillips *et al* 2006). However, in our case, lubrication or bearing-ball effects, levee formation, etc., do account for just a small RBP increment until the deposit separates into two clearly defined deposits. In the case of a binary mixture, there are in fact two avalanches competing against each other.

In our experiments, granulometric classes corresponding to inertial and viscous-like regimes were chosen to configure each mixture, in order to discern the effect the viscous-like flow of fine particles has on the inertial flow of coarse particles and vice versa. This competition leads to the prevalence of one behaviour over the other, depending on the relative content of each species, conferring the RBP a dual behaviour. On the one hand, if the inertial avalanche dominates, the RBP shows a very large increment, and the deposit can split into two parts: a distal, massive cluster of only coarse particles and a proximal, massive deposit consisting of only fine particles at the closest distance to the break in slope, followed by a layered, reverse-graded, mixed part of the deposit. However, if a gap does not form, the structure of the deposit remains the same with three very well differentiated zones: a pure-fine, proximal one; a reverse-graded, mixed, intermediate one; and purely coarse-particle, distal zone forming a single deposit. On the other hand, if the fine-grain, viscous-like avalanche dominates, the trend of RBP is towards diminishing. There is only one massive deposit with just two well defined zones: the proximal one of only fine particles attached to the reverse-graded mixed zone; the pure coarse grained deposit is absent.

Our findings show that dominance is critical, in the sense that there is no equilibrium state as a result of viscous-like-versus-inertial interactions. The transition is

always abrupt within a 7% (or less) variation of fine content. Additionally, for fixed-total-mass experiments (4 kg), we have found that the RBP of a binary avalanche is always greater than (or very similar to) the RBP of each corresponding monodisperse avalanches, depicted as a filled black square in figure 7. On the coarse-dominated side (inertial regime) before the transition, fine particles within interstices, formed by large particles, lubricate the interaction among large particles or between large particles and flume surfaces. On the other side, where fine particles are dominant (the whole behaviour is viscous-like), the RBP is larger than the one of only fine particles, due to the drag exerted by large inertial particles on the fine, “viscous-like” particles.

The formation of the distal deposit depends on a critical quantity of coarse particles, which allows the condensation of the deposit around a small initial cluster (a “seed”). This seed grows rapidly by braking and capturing subsequent coarse colliding particles. Note that now we are discussing in terms of coarse-particle content, instead of fine-particle content, because the distal cluster will form or not depending only on the density of scattered particles in the disperse cloud at the very front of the deposit.

By plotting the particle-diameter ratio as a function of critical fine-particle content, a power-law behaviour is obtained, as shown in figure 10. The critical content of fine particles diminishes as the particle-diameter ratio grows. This is due to the fact that a small quantity of large particles is not enough to constitute a well-defined, coarse-grain deposit, because the majority of them are scattered ahead of the massive deposit. This implies that the formation of the coarse-grain cluster is not possible until the coarse-particle density in the disperse cloud reaches a critical value that allows the formation of large clusters.

In figure 11, we show a phase diagram, corresponding to the five experiments reported in this paper. It can be observed that a deposit conformed by the main four sections of the deposit (FPD, RLG, GAP, and CPD) can only be obtained by a well-defined amount of coarse and fine particles in the original mixtures, and it is a function of the particle-diameter ratio. For a coarse-particle amount below and above those critical values, the final deposit is conformed only by the FPD and the RGLD. In all cases, a

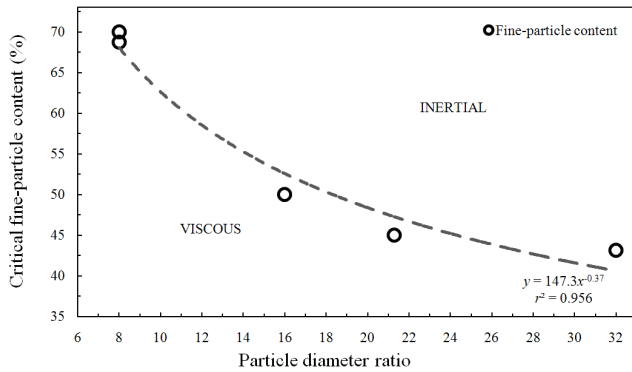


**Figure 10.** Critical amount of fine particles (%) needed to obtain the transition observed as a function of particle-diameter ratio. This line is also the border line for the viscous-like-to-inertial regime of the avalanche.

small amount of large particles is scattered beyond the tip of the massive, distal end of the deposit.

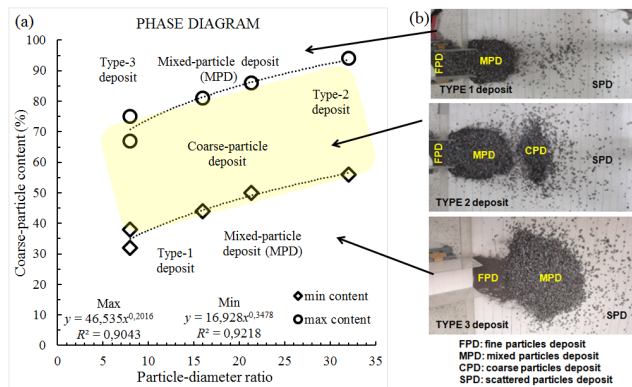


**Figure 11.** (a) Phase diagram showing the coarse-particle amount needed to obtain a coarse-particle deposit (CPD) as a function of particle-diameter ratio. A CPD is only allowed (for each particle-diameter ratio) inside the highlighted region. Outside this region, the deposit only shows a fine-grain deposit (FPD) closer to the break in slope and a mixed-grain deposit (RGLD) in front of it. (b) Example of deposits where it can be seen that the coarse-particle deposit forms only for a certain amount of coarse particles in the mixture. This quantity is highlighted and is a function of the particle-diameter ratio.

Remarkably, for mixtures in which two deposits form, (a coarse-grained, distal one, and an inversely graded proximal one) the morphology of the whole deposit strikingly resembles the hummocky deposits of the Parinacota debris avalanche in northern Chile, first described by Clavero *et al* (2002). As described by these authors, distal hummocks are placed ahead the avalanche front and are constituted mainly by coarse-grain rocks that show angled (instead of rounded) shapes and collision marks that we attribute to the clustering process we just described.

#### 4.4. Mobility

Mobility of rock avalanches is often measured using the ratio  $H/L$ . The height of fall,  $H$ , is measured vertically from the crest of the initial avalanche mass to the lowest point of reach, whereas the length of fall,  $L$ , is measured horizontally from the crest of the avalanche to the most distal point of reach (denoted as  $H_{\max}$  and  $L_{\max}$  in figure 1). The Fahrböschung angle,  $\theta$  (Shreve 1968, Hsu 1978), is defined as  $\theta = \tan^{-1}(H_{\max}/L_{\max})$ . We decided to characterize the mobility of our avalanches in this way because the travel angle,  $\alpha_G$ , defined as the angle between the centre of gravity of the initial mass and that of the deposit, is much less used, since it is very difficult to be determined in natural deposits (Bowman *et al* 2012).

In our case, since the deposit sometimes splits into two well-differentiated sequential deposits, the Fahrböschung angle is always measured from the rear of the initial granular pile to the tip of the most distal condensed or clustered front, which is the tip of the coarse particle deposit, CPD—when the deposit is split—or the MDP in all other cases.

The excess of runout or excess of travel distance  $L_e$  (Heim 1882, Hsu 1975, Corominas 1996, Shreve 1968, Legros 2002, Bowman *et al* 2012) is the difference between the distance travelled by the granular flow ( $L_{\max}$ ) and the one that may be expected ( $L_f$ ) for a mass sliding down an inclined plane, in the case when a “normal” coefficient of friction— $\tan(32^\circ) = 0.62$ —is considered:

$$L_f = \frac{H_{\max}}{\tan(32^\circ)};$$

$$L_e = L_{\max} - L_f$$

This friction coefficient (0.62) is expected in a purely frictional model when a block slides down an inclined plane, defined by Hsu (1975 and 1978). The percentage of the excess of runout plotted in figure 12 is then:

$$L_e\% = 100 \frac{L_{\max}}{L_f} - 100.$$

It can be seen that the excess runout is larger for mixtures in which the mass of large particles dominates over that of small particles. In order to compare the RBP of bi-disperse avalanches (figure 7) with that of monodisperse-avalanche (figure 8), it is important to note that both sets of experiments were performed using exactly the same material and the same experimental flume. As it can be seen, the fine-particle content (less than a critical quantity) modifies the mobility (or the RBP), with a tendency of increasing it. This can be due to the lubrication produced by interstitial fine particles, when coarse particles are the largest proportion by mass, or to coarse particles dragging fine particles, when coarse particles are a minority compared to the fine ones by mass. Instead, with a larger-than-critical mass of fine grains, collisions and friction tend

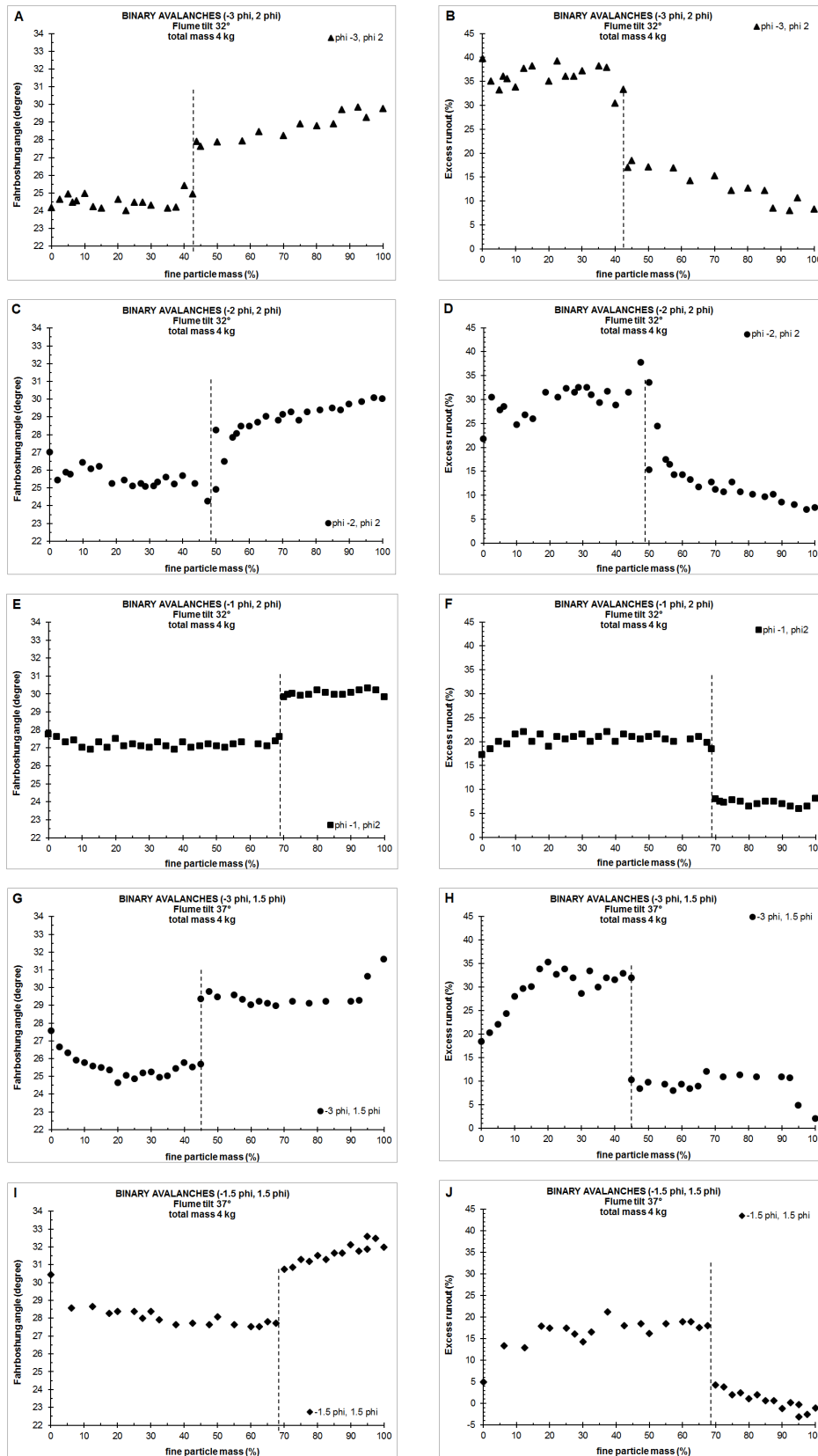


**Figure 12.** (a), (c), (e), (g), and (i): Föhn angle corresponding to avalanches containing the whole set of mixtures reported in table 1, as a function of the respective fine-particle content, showing the critical clustering transition pointed by the dashed line in each case. (b), (d), (f), (h), and (j): Excess runout (%) for the above-mentioned experiment.

to slow down the avalanche trapping the coarse particles between the fine ones, reducing the mobility and the runout of the flow, thus acting like a “sand-trap”.

## 5. Conclusions

We have reported the run from break point (RBP) of a binary-mixture avalanche as a function of its content of fine particles. Two competing behaviours, a viscous-like one, associated to fine particles, and an inertial one, associated to coarse particles, regulate the global behaviour of the mixed avalanche, depending on the proportion of each granulometric class within the mixture. We have found a tendency of increment of the RBP, which is produced when a small percent of fine particles are added to a coarse-grain avalanche, due to the lubrication among coarse grains and between coarse grains and the flume surface, produced by the presence of interstitial fine particles. This RBP increment saturates as more fine particles are added, until a sudden transition makes the RBP diminish abruptly to small values closer to those corresponding to the RBP of a monodisperse avalanche of fine particles. Here, the avalanche is dominated by a viscous-like behaviour, characteristic of these fine particles flowing down the inclined plane.

The sudden transition is caused by a clustering instability and occurs when the inertial-particle population, which overcomes the deposit of fine or mixed particles, reaches a critical amount, at which a new deposit of coarse particles condenses from the dispersed cloud. By looking at those clusters, formed from dispersed coarse particles at the very front, we suggest that clustering could be at the origin of some hummock-like structures formed at the front of long-runout, natural rock avalanches. The variation in the content of fine particles in the avalanching mixture required for the transition to occur is found experimentally to be lower than 7% by mass.

The formation of well-defined regions of only fine and only coarse particles and a mixed, reverse-graded region in the deposit shows that a complete segregation can be achieved for a large enough inertial contrast and/or flume length. The critical content of fines at the transition is related to the particle-size ratio as a power law for all the studied cases.

## Acknowledgments

We wish to thank the Geology Institute and LAIMA laboratory of Universidad Autónoma de San Luis Potosí, for sharing with us their facilities. This project was partially funded by CONACYT grant number 221961, Fondos Concurrentes UASLP and PhD-scholarship grant number 45697. We also wish to thank all the undergraduate students that helped us to perform the experiments.

## References

- [1] Andreotti B, Daerr A, Douady S 2002 Scaling laws in granular flows down a rough plane *Phys. Fluids* **14** 415–418
- [2] Bartali R, Sarocchi D, Nahmad-Molinari Y, Rodríguez-Sedano L A 2012 Estudio de flujos granulares de tipo geológico por medio del simulador multisensor GRANFLOW-SIM *Boletín de la Sociedad Geológica Mexicana* **64** 265–275
- [3] Bartali R, Sarocchi D, Nahmad-Molinari Y 2015 Stick–slip motion and high speed ejecta in granular avalanches detected through a multi-sensors flume *Eng. Geol.* **195** 248–257
- [4] Bordallo-Favela R A, Ramírez-Saíto A, Pacheco-Molina C A, Perera-Burgos J A, Nahmad-Molinari Y, Pérez G 2009 Effective potentials of dissipative hard spheres in granular matter *Eur. Phys. J. E* **28** 395–400
- [5] Bowman E T, Take W A, Rait K L, Hann C 2012 Physical models of rock avalanche spreading behavior with dynamic fragmentation *Can. Geotech. J.* **49** 460–476
- [6] Campbell C 2006 Granular material flows - an overview *Powder Tech.* **162** 208–229
- [7] Charrière M, Humair F, Froese C, Jaboyedoff M, Pedrazzini A, Longchamp C 2015 From the source area to the deposit: Collapse, fragmentation, and propagation of the Frank Slide *Geol. Soc. of Am. Bull.* **128** 332–351
- [8] Clavero J E, Sparks R S J, Huppert H E, Dade W B 2002 Geological constraints on the emplacement mechanism of the Parinacota debris avalanche, northern Chile *Bull. Volcanol.* **64** 40–54
- [9] Corominas J 1996 The angle of reach as a mobility index for small and large landslides *Can. Geotech. J.* **33** 260–271
- [10] Fauque L, Strecker M R, 1988 Large rock avalanche deposits (Sturzströme, sturzstroms) at Sierra Aconquija, northern Sierras Pampeanas, Argentina. *Eclogae Geologicae Helveticae* **81** 572–599
- [11] Glicken H 1996 Rockslide-debris avalanche of May 18, 1980, Mount St. Helens volcano, Washington. *United States Geological Survey Open File Report* **96** 677
- [12] Goldhirsch I, Zanetti G, 1993 Clustering instability in dissipative gases *Phys. Rev. Lett.* **70** 1619
- [13] Goujon C, Thomas N, Dalloz-Dubrujeau B 2003 Monodisperse dry granular flows on inclined planes: Role of roughness *Eur. Phys. J. E* **11** 147–157
- [14] Goujon C, Dalloz-Dubrujeau B, Thomas N 2007 Bidisperse granular avalanches on inclined planes: A rich variety of behaviors *Eur. Phys. J. E* **23** 199–215
- [15] Heim A, 1882 Der Bergsturz von Elm. *Zeitschrift der Deutschen Geologischen Gesellschaft* **34** 74–115
- [16] Hungr O, Evans S G 2004 Entrainment of debris in rock avalanches: An analysis of a long run-out mechanism *Geol. Soc. of Am. Bull.* **116** 1240–1252
- [17] Hsü K J 1975 Catastrophic debris streams generated by rock falls *Geol. Soc. of Am. Bull.* **86** 129–140
- [18] Hsü K J 1978 Albert Heim, observations on landslides and relevance to modern interpretations *Rockslides and avalanches, 1 (Developments in Geotechnical Engineering vol 14A)* ed B Voight (Amsterdam: Elsevier) pp 71–92
- [19] Huerta D A, Sosa V, Vargas M C, Ruiz-Suárez J C 2005 Archimede’s principle in fluidized granular systems *Phys. Rev. E* **72** 031307
- [20] Kokelaar B P, Graham R L, Gray J M N T, Vallance J W 2014 Fine-grained linings of leveed channels facilitate runout of granular flows *Earth and Planetary Sci. Lett.* **385** 172–180
- [21] Legros F 2002 The mobility of long-runout landslides. *Eng. Geol.* **63** 301–331
- [22] Linares-Guerrero E, Goujon C, Zenit R 2007 Increased mobility of bidisperse granular avalanches *J. Fluid Mech.* **593** 475–504
- [23] McColl S T, Davies T R 2011 Evidence for a rock-avalanche origin for ‘The Hillocks’ “moraine”, Otago, New Zealand *Geomorphology* **127** 216–224
- [24] Mikkelsen R, van der Meer D, van der Weele K, Lohse D 2002 Competitive Clustering in a Bidisperse Granular Gas *Phys. Rev. Lett.* **89** 214301
- [25] Mikkelsen R, van der Weele K, van der Meer D, van Hecke M, Lohse

- D, 2005 Small-number statistics near the clustering transition in a compartmentalized granular gas *Phys. Rev. E* **71** 041302
- [26] Olafsen J S, Urbach J S 1998 Clustering, Order, and Collapse in a Driven Granular Monolayer *Phys. Rev. Lett.* **81** 4369
- [27] Pacheco-Vázquez F, Ruiz-Suárez J C 2009 Sliding through a superlight granular medium *Phys. Rev. E* **80** 060301(R)
- [28] Paguican E M R, van Wyk de Vries B, Lagmay A 2014 Hummocks: how they form and how they evolve in rockslide-debris avalanches *Landslides* **11** 67-80
- [29] Perera-Burgos J A, Pérez-Ángel G, Nahmad-Molinari Y 2010 Diffusivity and weak clustering in a quasi-two-dimensional granular gas *Phys. Rev. E* **82** 051305
- [30] Phillips J C, Hogg A J, Kerswell R R, Thomas N H, 2006 Enhanced mobility of granular mixtures of fine and coarse particles *Earth and Planetary Sci. Lett.* **246** 466–480
- [31] Pouliquen O 1999 Scaling laws in granular flows down rough inclined planes *Phys. Fluids* **11** 542
- [32] Robinson T R, Davies T R H, Reznichenko N V, De Pascale G P, 2015 The extremely long-runout Komansu rock avalanche in the Trans Alai range, Pamir Mountains, southern Kyrgyzstan *Landslides* **12** 523–535
- [33] Sapozhnikov M V, Aranson I S, Olafsen J S 2003 Coarsening of granular clusters: Two types of scaling behaviors *Phys. Rev. E* **67** 010302(R)
- [34] Shreve R L 1968 The Blackhawk Landslide *GSA Special Papers* **108** 1-48
- [35] Siebert L 1984 Large volcanic debris avalanches: Characteristics of source areas, deposits, and associated eruptions *J. of Volcanol. and Geothermal Research* **22** 163-197
- [36] Ui T 1983 Volcanic dry avalanche deposits - Identification and comparison with nonvolcanic debris stream deposits *J. of Volcanol. and Geothermal Research* **18** 135-150
- [37] Van Gassen W, Cruden D M 1990 Momentum transfer and friction in the debris of rock avalanches *Can. Geotech. J.* **27** 698-699
- [38] Wentworth C K 1922 A Scale of Grade and Class Terms for Clastic Sediments *J. Geology* **30** 377–392
- [39] Yang Q, Cai F, Ugai K, Yamada M, Su Z, Ahmed A, Huang R, Xu Q 2011 Some factors affecting mass-front velocity of rapid dry granular flows in a large flume *Eng. Geol.* **122** 249–260